

# Effects of heat-treatment methods on cytocompatibility and mechanical properties of dental products 3D-printed using photopolymerized resin

Na-Eun Nam <sup>a</sup>, Na-Kyung Hwangbo <sup>b</sup>, Gan Jin <sup>c</sup>, June-Sung Shim <sup>c</sup>, Jong-Eun Kim <sup>c,\*</sup>

<sup>a</sup> BK21 FOUR Project, Department of Prosthodontics, Yonsei University College of Dentistry, Korea

<sup>b</sup> Department of Orofacial Pain and Oral Medicine, Yonsei University College of Dentistry, Korea

<sup>c</sup> Department of Prosthodontics, College of Dentistry, Yonsei University, Korea

## Abstract

**Purpose:** The purpose of this study was to test heat-treatment methods for improving the cytocompatibility of dental 3D printable photopolymer resins.

**Methods:** Nextdent C&B resin and a digital light processing 3D printer were used to print all specimens, which were divided into seven groups as follows: 1-month storage at controlled room temperature, 20 to 25 °C (RT), 24-hour storage at RT, 24-hour storage in RT water, 1-min immersion in 80 °C water, 1-min immersion in 100 °C water, 5-min immersion in 100 °C water, and autoclaving. Cell viability tests, cytotoxicity tests, and confocal laser scanning microscopy were performed to analyze the cytocompatibility of the 3D-printed resin. Fourier-transform infrared spectroscopy was performed after heat-treatment to determine the degree of conversion (DC).

**Results:** Immersing printed resin samples in 100 °C water for 1 or 5 min after the curing process was an effective method for increasing cytocompatibility by inducing the preleaching of toxic substances such as unpolymerized monomers, photoinitiators, and additives. Moreover, the DC can be increased by additional polymerization without affecting the mechanical properties of the material.

**Conclusions:** Immersing the printed photosensitive dental resins in 100 °C water for 5 min is a suitable method for increasing cytocompatibility and the DC.

**Keywords:** Additive manufacturing, Cell viability, Cytotoxicity, Residual monomer, Threedimensional printing

Received 27 December 2021, Accepted 14 March 2022, Available online 14 May 2022

## 1. Introduction

The introduction of computer-aided design/computer-aided manufacture (CAD/CAM) systems into dental restoration production has resulted in a gradual increase in the proportion of dental prostheses produced using digital dentistry technology[1,2]. CAD/CAM systems reduce the errors that occur in conventional prosthesis fabrication techniques and are cost-effective[1]. Because of these advantages, CAD/CAM systems have replaced the conventional techniques used in medical care[3].

Subtractive or additive methods can be used to manufacture prostheses designed using CAD software[4]. Milling technology, which cuts prefabricated blocks or disks into a desired shape, enables prosthesis fabrication with high mechanical performance and accuracy and good biological properties[5,6]. However, manufactur-

ing complex shapes by using subtractive methods is difficult, and the consumption of materials and milling burs is considerable[7–9]. In contrast, additive methods, such as 3D printing, do not use drills or burs, avoid wear-related problems, and can produce more complex shapes or designs, such as the emptying of internal structures[5,7]. Thus, the popularity of additive methods for temporary crowns, implant surgical guides, and dental models is increasing[10,11].

Unlike blocks used in subtractive manufacturing that are marketed after polymerization at high temperatures and pressures[12], the residual monomer toxicity of acrylic resins used in additive manufacturing is considered a major disadvantage[13–15]. Printable photosensitive resins consist of monomers mostly based on (meth) acrylates, photoinitiators (PIs), and additives[16,17]. The ultraviolet (UV) laser or the light emitted from 3D printers activates the PI of the liquid resin[18] to produce free radicals that change the resin from a viscous to a hard state and then initiate the additional methacrylate reaction[19].

After the resin photocuring process is performed, although the cross-linked polymer matrix may not have been leached, unreactive monomers, short-chain polymers, PIs, and additive residues become

DOI: [https://doi.org/10.2186/jpr.JPR\\_D\\_21\\_00345](https://doi.org/10.2186/jpr.JPR_D_21_00345)

\*Corresponding author: Jong-Eun Kim, Department of Prosthodontics, College of Dentistry, Yonsei University, Yonsei-ro 50-1, Seodaemun-gu, Seoul 03722, Korea.

E-mail address: [gomyou@yuhs.ac](mailto:gomyou@yuhs.ac)

Copyright: © 2022 Japan Prosthodontic Society. All rights reserved.

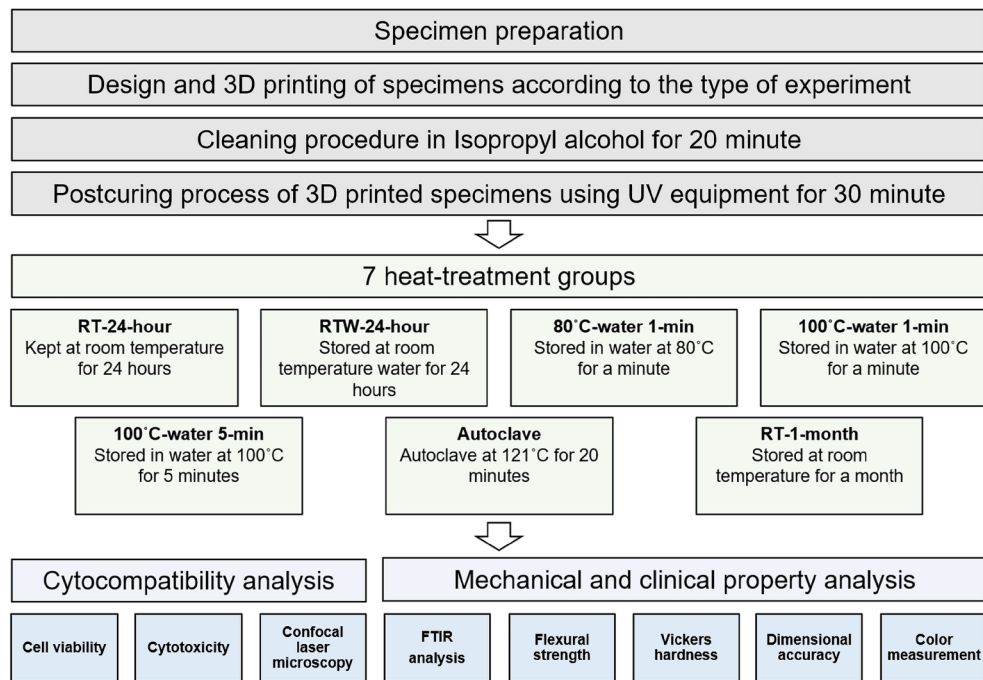


**Fig. 1.** Overall workflow of the experiments

prone to leaching when the printed resin is stored in an aqueous medium. Therefore, these leachates can reduce the biocompatibility of the material[20]. In toxicity studies, methacrylate monomers have been shown to exhibit aquatic toxicity, genotoxicity, and embryotoxicity[21–23]. These cytotoxic effects can affect cellular lipid metabolism and even induce apoptosis or necrosis[24,25]. In previous studies, unpolymerized monomers induced irritation that can lead to pulpitis, glossitis, or stomatitis[26]. Therefore, an effective post-process that reduces the toxicity of 3D-printed resin prostheses is required.

Isopropanol (IPA) can reduce cytotoxicity by removing uncured monomers from the surface of the 3D-printed resin[23]. However, extending the washing time with IPA may dissolve the monomer and swell the polymer. During this swelling process, IPA molecules can gradually diffuse into the polymer matrix, loosening the polymer network and reducing its mechanical strength[27,28]. In a previous study in which the effect of the postcuring time on resin biocompatibility was investigated, even with an increasing postcuring time, cell viability was found to decrease as the incubation time increased[29]. In previous studies, a wax coating was applied to the resin to delay and reduce toxic compound leaching in 3D-printed resins[30,31]. However, in the case of dental prostheses, this coating can be easily removed via occlusal adjustment or mastication in the oral cavity, and the coating thickness may negatively affect the fit. Methods for reducing the residual monomer content of acrylic resins have been reported, such as immersing them in hot water or irradiating them using microwaves[32–34]. However, for photopolymerized 3D-printed resins, the method of increasing the cytocompatibility of the material by enhancing the reductions of residual monomers and resin compounds has not been explored in previous studies.

The purpose of this study was to develop a method for lowering cytotoxicity by performing additional heat-treatments, such as

immersing the specimen in hot water or using an autoclave after cleaning and postcuring the 3D-printed dental crown and bridge resin. The effects of this process on the accuracy, color tone, and mechanical properties of the printed prostheses were evaluated. The null hypothesis was that biocompatibility, color stability, accuracy, and mechanical properties would not differ with the heat-treatment method applied to 3D-printed dental resins.

## 2. Materials and Methods

The overall workflow of the experiments is shown in **Figure 1**.

### 2.1. Specimen Preparation

Universal CAD software (Rhino<sup>®</sup> version 5, Robert McNeel & Associates, Seattle, WA, USA) was used to design the specimen, and the design file was exported in the STL format. The digital light processing (DLP) resin from NextDent C&B (NextDent, Soesterberg, The Netherlands) was used as the material for the specimen output in 3D printing, and all specimens were printed using a DLP 3D printer (NextDent 5100, 3D Systems, NextDent). As per the instructions of the manufacturer, the uncured resin remaining on the specimen surface was washed with 3D printing washer (Twin Tornado, MEDIFIVE, Incheon, Korea) and 90% isopropyl alcohol for 10 min. Postcuring was performed for 30 min using curing equipment (Form Cure, Formlabs, Berlin, Germany) at a UV intensity of 220  $\mu\text{W}/\text{cm}^2$  UV intensity and an internal temperature of 60 °C. The completed specimens were kept in darkness and divided into groups based on their heat-treatment method: 1-month storage at controlled room temperature, 20 to 25 °C (RT), 24-hour storage at RT, 24-hour storage in room temperature water (RTW), 1-min immersion in 80 °C water, 1-min immersion in 100 °C water, 5-min immersion in 100 °C water, and autoclaving at 121 °C for 15 min under 2 bar (autoclave). **Figure 1** presents the heat-treatment groups.

## 2.2. Cell Viability Analysis

Cell viability and cytotoxicity analyses were performed to determine the cytocompatibility of the 3D-printed specimens based on the heat-treatment process. For the cytocompatibility test, five specimens, having a diameter of 9.5 mm and a thickness of 2 mm, per group ( $n = 5$ ) were printed, and heat-treatment was performed on each group, with all specimens sterilized using ethylene oxide gas to prevent surface contamination. Primary human gingival fibroblasts (PCS-201-018, ATCC, Manassas, VA, USA) were used in this experiment. Cell culture was performed in a cell culture dish by using Dulbecco's modified Eagle's medium (WelGene, Daegu, Republic of Korea) supplemented with penicillin/streptomycin (100X, WelGene), MEM nonessential amino acid solution (100X, WelGene), and 10% fetal bovine serum (Thermo Fisher Scientific, Waltham, MA, USA) at 37 °C in an atmosphere with 5% CO<sub>2</sub> and 95% air and 100% relative humidity. The cell culture media were replaced with a fresh medium every 2 or 3 days, and the cells were treated with 0.21% trypsin-ethylenediaminetetraacetic acid (Trypsin-EDTA, 1X, WelGene) solution when they reached 85–90% confluency. The separated cells were centrifuged to remove the old medium and Trypsin-EDTA solution, and the cells were diluted to a density of  $5 \times 10^4$  cells/ml in the fresh medium.

The cell viability was evaluated using a CELLOMAX™ viability kit (Precaregene, Hanam, Kyungido, Korea) based on tetrazolium salt (2-[2-methoxy-4-nitrophenyl]-3-[4-nitrophenyl]-5-[2,4-disulphophenyl]-2H-tetrazolium) and monosodium salt (WST-8; Precaregene). First, the circular 3D-printed resin from each group was distributed on 48-well plates. Gingival fibroblasts were trypsinized and seeded into the 48-well plates with each 3D-printed resin sample at a density of  $5 \times 10^4$  cells/well. After 24, 48, and 72 h of incubation, 50 µL of the CELLOMAX™ solution (CELLOMAX™ viability assay kit, Precaregene) was added to the 48-well plate of the specimen. Wells in which only cells without specimens were cultured were used as a positive-control group and incubated for 90 min at 37 °C as per the instructions of the manufacturer. From each well, 100-µL aliquots of the media were subsequently transferred to a 96-well plate, and their optical density at 450 nm was recorded using a microplate reader (VERSA max, Molecular Devices, Sunnyvale, CA, USA). The percentage of cell viability was calculated using the following equation:

$$\text{Cell viability (\%)} = \left( \frac{O.D_{\text{test sample}} - O.D_{\text{blank}}}{O.D_{\text{control}} - O.D_{\text{blank}}} \right) \times 100.$$

## 2.3. Cytotoxicity Analysis

The cytotoxicity of the 3D-printed resin on gingival fibroblasts was measured using a lactate dehydrogenase (LDH) release assay (Quanti-LDH™ Cytotoxicity Assay Kit, BIOMAX, Seoul, Korea) as per the instructions of the manufacturer. Gingival fibroblasts were seeded on the 48-well plate of each 3D-printed resin at a density of  $5 \times 10^4$  cells/well. After 24, 48, and 72 h, 20 µL of the culture medium was collected and centrifuged at 7000 rpm for 3 min. Then, 10 µL of the obtained supernatant was transferred to a new 96-well plate, to which 100 µL of the LDH substrate mixture was added. After 30 min of incubation at RT, the absorbance of the resultant solution was measured at 450 nm. For the cytotoxicity assay, the medium was not changed until after 72 h. The percentage of cytotoxicity was calculated using the following equation:

$$\text{Cytotoxicity (\%)} =$$

$$\left[ \frac{(OD_{\text{cells with 3D printed resin}} - OD_{\text{background control}}) - (OD_{\text{low control}} - OD_{\text{background control}})}{(OD_{\text{high control}} - OD_{\text{background control}}) - (OD_{\text{low control}} - OD_{\text{background control}})} \right] \times 100,$$

where the background control was the medium only, the low control was the culturing of the supernatants of the fibroblast cells only, and the high control was the culturing of the supernatants of the fibroblast cells after homogenization of the cell lysis buffer.

## 2.4. Cytoskeleton Staining and Confocal Laser Scanning Microscopy

After the cells were cultured for 24 h on the specimens of each group, the specimens were washed thrice with phosphate buffered saline (PBS), and the cells were fixed with 4% paraformaldehyde in PBS for 15 min at RT. The specimens were then washed three more times and permeabilized with 0.1% Triton™ X-100 in PBS for 15 min. Finally, the specimens were washed thrice with PBS. For cytoskeletal quantification, the cytoskeleton was bound to β-actin and fluorescently stained with phalloidin (Alexa Fluor 488 Phalloidin, Invitrogen, Thermo Fisher Scientific) as per the instructions of the manufacturer. The specimens were then mounted on an antifade mounting medium (VECTASHIELD, Vector Laboratories, Burlingame, CA, USA) and scanned by performing confocal laser scanning microscopy (CLSM; LSM 700, Carl Zeiss Microscopy, Jena, Germany). Z-stack continuous capture images were used to determine the coexpression levels.

## 2.5. Degree of Conversion

Fourier transform infrared spectroscopy (FTIR) was performed to identify the functional groups present in the 3D-printed resin. Five specimens, having a diameter of 10 mm and a thickness of 2 mm, were prepared per group. After the heat-treatment of the specimens, infrared spectra were acquired using a Vertex 70 FTIR spectrometer (Bruker, Karlsruhe, Germany). The spectra were recorded in the absorbance mode using a diamond crystal plate and obtained with a resolution of 4 cm<sup>-1</sup> in the spectral region of 500–4000 cm<sup>-1</sup>. The experiment was performed three times for each specimen. In each spectrum, the heights of the absorption bands of the aliphatic and aromatic C=C bonds were measured at 1637 cm<sup>-1</sup> and 1608 cm<sup>-1</sup>, respectively. The degree of conversion (DC) was determined according to the following equation:

$$DC (\%) = \left\{ 1 - \frac{1637 \text{ cm}^{-1} / 1608 \text{ cm}^{-1} \text{ Peak height (cure)}}{1637 \text{ cm}^{-1} / 1608 \text{ cm}^{-1} \text{ Peak height (uncure)}} \right\} \times 100.$$

## 2.6. Flexural Strength

The flexural strength was tested using a universal tester (Model 3366, Instron Corporation, Norwood, MA, USA). A 10-kN-loaded cell with a crosshead speed of 0.75 mm/min<sup>-1</sup> was used based on the ISO-4049 standard[35]. In the mechanical property tests, a bar specimen ( $n = 15$  per group) was designed with a length of 25 mm, width of 2 mm, and thickness of 2 mm, according to the ISO-10477 standard[36]. Before the experiment, measurements were performed to an accuracy of 0.001 mm using digital calipers, and the flexural strength was measured. Two round supports separated by 20 mm were used for the fracture test, and the fracture load was measured in Newtons. The flexural strength ( $\sigma$ ) was calculated in megapascals

using the following equation:

$$\sigma = 3FI / 2bh^2,$$

where  $F$  is the breaking load in Newtons,  $I$  is the distance between the supports in millimeters,  $b$  is the specimen width in millimeters, and  $h$  is the specimen height in millimeters.

### 2.7. Vickers Hardness Test

The Vickers hardness was measured using disk-shaped specimens with a diameter of 9 mm and thickness of 2 mm, which were prepared using water-cooled polishing with a 1200-grit carbon paper. Five specimens ( $n = 5$ ) from each group were measured three times, and the average of these measurements was used. The indentation was produced by applying a 200 g (1.96 N) load for 15 s using a micro Vickers hardness tester (HMV-G31ST, Shimadzu, Kyoto, Japan) [37]. The Vickers hardness was calculated using the following equation:

$$HV = 1.854 \left( \frac{F}{D^2} \right),$$

where  $F$  is the breaking load in Newtons and  $D^2$  is the indentation area (measured in square millimeters).

### 2.8. Dimensional Accuracy

To determine the effects of the heat-treatment on the accuracy of the specimen, dental CAD software (Exocad DentalCAD, Exocad, Darmstadt, Germany) was used to design a three-unit bridge for teeth 4, 5, and 6 (**Fig. S1**). The completed file was exported in the STL format. All specimens ( $n = 5$  per group) were fabricated using a DLP 3D printer (NextDent 5100, 3D Systems, NextDent) and the crown and bridge resin (NextDent C&B), with five printed specimens for each group. Each printed specimen was scanned using a tabletop scanner (T500, Medit, Seoul, Korea), and the STL file was applied to a 3D analysis software program (Geomagic Control X, 3D Systems, NextDent). The outer surfaces of the STL files were evaluated in three dimensions by comparing them with those of the CAD design files used as reference data.

The trueness and precision can be analyzed using the ISO-5725-1 standard, where trueness represents how close the sample data are to the reference values, and precision denotes how close the values are between the comparison data. A best-fit algorithm was used to perform 3D analyses of the trueness of the obtained data; it has been used as a method for evaluating accuracy in several previous studies. The error between the reference and comparison data was quantified as the root-mean-square error (RMSE) and presented as a map with colors based on the tolerance ranges. The RMSE is a type of mean calculated as the square root of the mean square; it can present the error index in units similar to the actual value and is commonly applied to measure the volume and shape variability of surfaces[38]. The RMSE values were calculated using the following formula:

$$RMSE = \frac{1}{\sqrt{n}} \times \sqrt{\sum_{i=1}^n (\chi_{1,i} - \chi_{2,i})^2},$$

where  $\chi_{1,i}$  is the measurement point of the reference,  $\chi_{2,i}$  is the measurement point of the dataset, and  $n$  is the total number of points measured in each analysis.

### 2.9. Color Measurement

To evaluate the color changes in the specimens according to the heat-treatment process, the color of each untreated specimen was examined after 3D printing and the completion of the heat-treatment process. Specimens ( $n = 5$  per group) with a diameter of 9 mm and a thickness of 2 mm were prepared for each group. The color of each finished specimen was evaluated three times using a colorimeter (CR-321 Chromameter, Minolta, Osaka, Japan), and the average value of the three measurements for each specimen was used. The color change was evaluated by applying the  $L^*$ ,  $a^*$ , and  $b^*$  values measured at each point to the CIEDE2000 formula ( $\Delta E_{00}$ ):

$$\Delta E_{00} = \sqrt{\left( \frac{\Delta L}{K_L S_L} \right)^2 + \left( \frac{\Delta C}{K_C S_C} \right)^2 + \left( \frac{\Delta H}{K_H S_H} \right)^2 + R_T \left( \frac{\Delta C}{K_C S_C} \right) \left( \frac{\Delta H}{K_H S_H} \right)}.$$

### 2.10. Statistical Analysis

Statistical analyses were performed using the SPSS software (version 25, IBM, Armonk, NY, USA). The normality of all data was confirmed by performing the Shapiro-Wilk test. The data from the cell viability and cytotoxicity assays were analyzed by applying the two-way analysis of variance (ANOVA) to confirm the two-way interaction between the heat-treatment method and incubation time. The one-way ANOVA was used to identify the differences between the heat-treatment method groups and the incubation times in the obtained data. The data on the DC, color difference, flexural strength, and Vickers hardness were analyzed using the one-way ANOVA. The significance level was calculated, and Scheffe's test was performed as a post-test ( $\alpha=0.05$ ). The mean and standard deviation values were calculated and evaluated for each group. Paired-sample t-tests were performed with a significance cutoff of  $\alpha=0.05$  to identify the dimensional changes in the three-unit bridge before and after the heat-treatment process.

## 3. Results

### 3.1. Cell Viability Evaluation

The two-way ANOVA of the incubation time and heat-treatment method for cell viability (**Fig. S2, Table S1**) indicated significant main effects of the heat-treatment method ( $F=96.701$ ,  $p<0.001$ ) and incubation time ( $F=5.078$ ,  $p=0.008$ ). However, it also indicated that there was no significant effect between the heat-treatment method and incubation time ( $F=1.850$ ,  $p=0.053$ ).

To determine the differences in the cell viability for the different heat-treatment methods, one-way ANOVA was performed to compare the average standard deviations of the cell viability (**Fig. S3, Table S2**). No intergroup difference was observed for the cell viabilities after 24 h of incubation in the RT-1-month, RT-24-hour, RTW-24-hour, and 80-°C-water 1-min groups. However, for the autoclave, 100-°C-water 1-min, and 100-°C-water 5-min groups that had heat applied to them, the cell viabilities after 24 hours of incubation were 83.5±16.6%, 89.1±15.2%, and 80.3±14.5%, respectively, which were



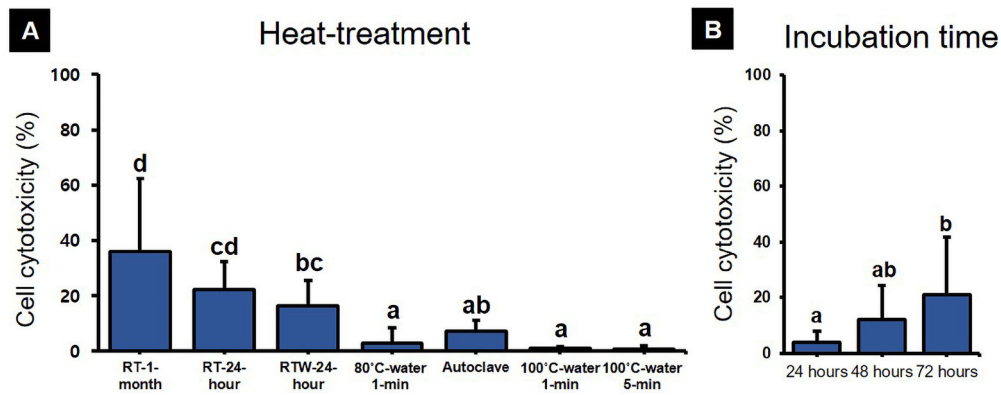


**Fig. 2.** Two-way ANOVA results of cytotoxicity. A) Cytotoxicity based on heat-treatment method. B) Cytotoxicity based on incubation time. The data are the mean and standard-deviation values. Different lower-case letters indicate significant intergroup differences ( $p < 0.05$ ).

significantly higher than those in the remaining groups. After 48 h of incubation, the cell viability rates in the autoclave, 100-°C-water 1-min, 100-°C-water 5-min groups were  $90.2 \pm 17.4\%$ ,  $99.9 \pm 28.6\%$ , and  $86.4 \pm 9.1\%$ , respectively, which were significantly higher than the other groups. Cell viabilities after 72 h of incubation of the 100-°C-water 1-min and 100-°C-water 5-min groups were significantly higher than the other groups, at  $87.7 \pm 14.3\%$  and  $99.5 \pm 14.4\%$ , respectively.

### 3.2. Cytotoxicity Test

The two-way ANOVA of the incubation time and heat-treatment method for cytotoxicity (**Fig. 2, Table S3**) indicated significant main effects of the heat-treatment method ( $F=320.900$ ,  $p < 0.001$ ) and incubation time ( $F=306.837$ ,  $p < 0.001$ ), as well as a significant interaction between the heat-treatment method and incubation time ( $F=73.092$ ,  $p=0.001$ ).

To determine the differences in cytotoxicity according to the heat-treatment methods, one-way ANOVA was performed to compare the average standard deviations of cytotoxicity (**Fig. S4, Table S4**). After 48 and 72 h of incubation, the cytotoxicity did not increase in the autoclave, 100-°C-water 1-min, and 100 °C-water 5-min groups. However, in the 80 °C water 1-min group, the cytotoxicity increased significantly to  $8.6 \pm 6.8\%$  after 72 h, and in the RT-1-month, RT-24-hour, and RTW-24-hour groups, it tended to increase at both 48 and 72 h. After 72 h of incubation, the cytotoxicity was highest in the RT-1-month group, followed by the RT-24-hour and RTW-24-hour groups, at  $69.8 \pm 4.1\%$  and  $30.9 \pm 1.8\%$ , respectively.

### 3.3. CLSM Analysis

When the cells were cultured on the specimens prepared for each group for 24 h, the cytoskeleton fluorescently stained with phalloidin, and the cell morphology of the specimen surface was identified using confocal laser scanning (**Fig. 3**). In the RT-1-month, RT-24-hour, and RTW-24-hour groups, relatively few cells were attached to the surface of each specimen, and cell malformation was observed. Conversely, the 100 °C-water 1-min and 100 °C-water 5-min groups were more attached to the specimens in the autoclave. Comparisons of the morphology of the blue-stained multinucleate cells and green-stained cytoplasm and filopodia indicated that the cells in the autoclave, 100 °C-water 1-min and 100 °C-water 5-min

groups developed well into an elongated shape. Additionally, more cell-to-cell contacts were detected on the surfaces of the specimens in these groups than in the RT-1-month, RT-24-hour, and RTW-24-hour groups. Therefore, the CLSM results were consistent with the cell viability and cytotoxicity evaluation results.

### 3.4. Degree of conversion

The results for the DCs are depicted in **Figure 4A** and **Table S5**. The DC of the 3D-printed resin used in the experiments varied depending on the heat-treatment method ( $p < 0.001$ ). The DC increased significantly in the 80 °C-water 1-min and the 100 °C-water 1-min groups compared with the RT-24-hour group. The DC was the highest in the 100 °C water 5-min group, at  $76.0 \pm 1.9\%$ .

### 3.5. Flexural Strength

The flexural strengths of the different groups are shown in **Figure 4B** and **Table S6**. The flexural strength of the 3D-printed resin used in the experiments varied with the heat treatment method. No significant differences in the flexural strength were found among the RT-1-month, RT-24-hour, RTW-24-hour, 80 °C-water 1-min, 100 °C-water 1-min, and 100 °C-water 5-min groups. However, the flexural strength was significantly lower in the autoclave group at  $95.3 \pm 16.9$  MPa.

### 3.6. Vickers Hardness Test

The changes in the Vickers hardness according to the heat-treatment method are presented in **Figure 4C** and **Table S7**. There was no difference in the surface hardness according to the heat treatment method.

### 3.7. Dimensional Accuracy

Five three-unit bridges were printed and scanned for each group to determine the trueness before and after heat treatment and to obtain each RMSE value (**Fig. 5A, Table S8**). The overall deviation distribution is displayed as a color map (**Fig. S5**). One-way analysis of variance was performed to identify the differences between the groups. There were no significant differences in the RMSE values between the groups before and after the heat treatment. The

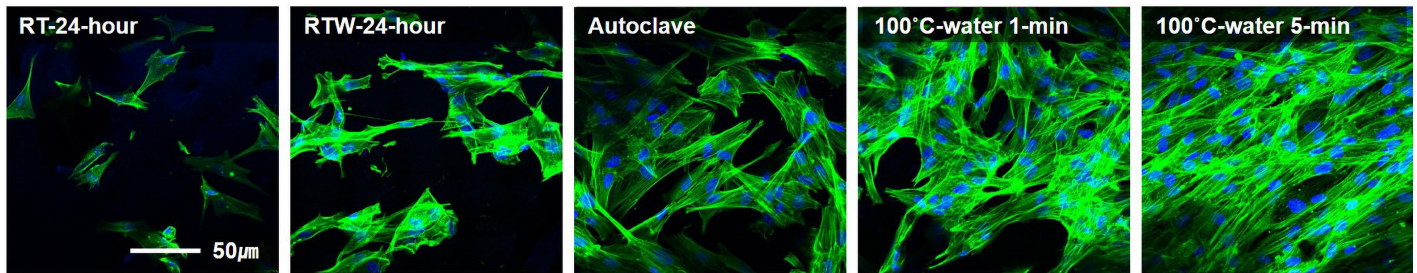


**Fig. 3.** Confocal laser microscopy images of human gingival fibroblasts cultured on specimens. The heat-treatment method was found to affect cell growth. In the case of the groups that were heat-treated at 100 °C water, the cell growth was considerably high. Cell malformations were observed in the room temperature storage groups (RT-24-hour and RTW-24-hour).

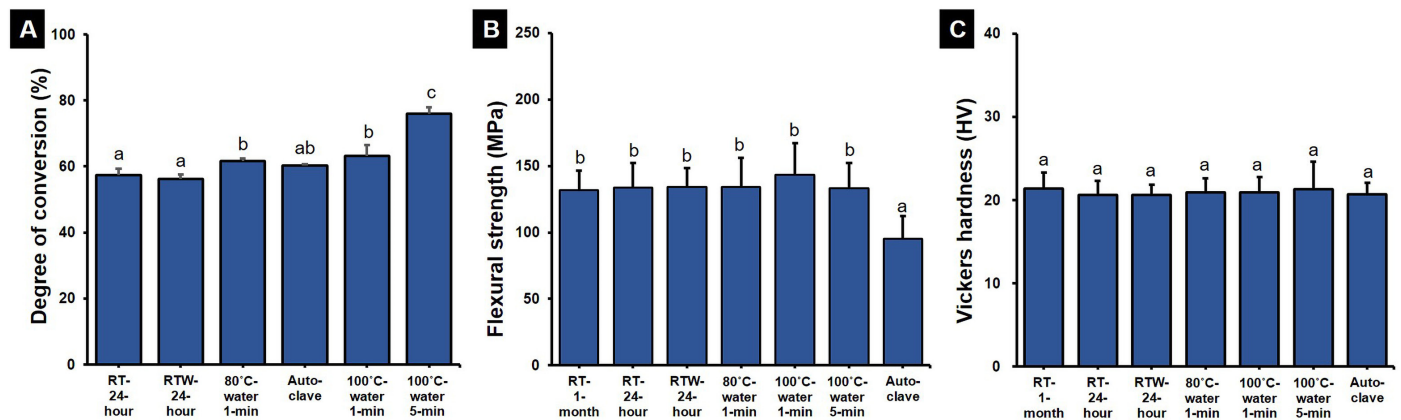


**Fig. 4.** Mechanical property results. A) DC, B) Flexural strength, and C) Vickers hardness of the 3D-printed resins based on post-treatment method.

paired-samples *t*-test indicated the absence of significant differences among all groups, except for the RTW-24-hour group.

### 3.8. Color Difference

The  $\Delta E_{00}$  value was calculated to determine color changes in the specimens according to the heat-treatment method, and the differences between the groups were determined using one-way ANOVA (Figs. 5B, 6, and Table S9). The color difference was the lowest ( $\Delta E_{00}=0.72$ ) for the RT-24-hour group, and there were no significant differences between those of the RT-1-month, RTW-24-hour, 80 °C-water 1-min, and 100 °C-water 1-min groups. The average color difference in the 100 °C-water 5-min group was  $\Delta E_{00}=1.63$ , which was significantly higher than that in the RT-24-hour group. The color difference in the autoclave group specimens was highest at  $\Delta E_{00}=6.7$ .

## 4. Discussion

In this study, hot-water immersion treatment and autoclaving were applied to 3D-printed crowns and bridge resins. The aim of this study was to determine whether the cytotoxicity of 3D-printed crowns and bridge resins could be reduced and whether cell viability could be increased. The effects of the heat treatment method on the mechanical properties, color stability, and dimensional accuracy were also evaluated. The experiments indicated that biocompatibility was significantly greater in the group with 3D-printed resin stored in water than in the group stored at RT. Moreover, increasing the

water temperature to 80 °C and 100 °C could further increase cytocompatibility. Autoclaving did not affect the dimensional accuracy of the 3D-printed three-unit bridge, but significantly affected its color stability and flexural strength. However, there were no differences in the color stability, dimensional accuracy, or mechanical properties among the other groups. Therefore, the null hypothesis is partially accepted.

The cell viability on the 3D-printed resin was found to be significantly lower in the RT-24-hour and RT-1-month groups with no treatment than in the other groups, and the cytotoxicity was significantly higher than in the other groups. In addition, as the incubation time increased from 24 h to 48 h to 72 h, the cytotoxicity significantly increased, indicating that the biocompatibility of the material decreased. This is consistent with the findings of Kim et al.[29], where 3D-printed crowns and bridge resins exhibited increased cytotoxicity after 48 h of incubation compared to that after 24 h. This is also similar to the results obtained by Bayarsaikhan et al.[39], who found that the cytotoxicity rapidly increased as the incubation time increased from 24 to 48 to 72 hours. The unpolymerized monomers in the deeper layers of the printed resin leached over time, inducing a cytotoxic effect[40], and resin-based restorative materials have been reported to exhibit leaching that induces cytotoxicity by 2 weeks[41]. As the incubation time increased to 72 h, the cytotoxicity probably increased rapidly owing to the accumulation of leaching among the decomposed compounds[42]. In the present study, cytotoxicity was significantly lower in the RTW-24-hour group than in the RT-24-hour

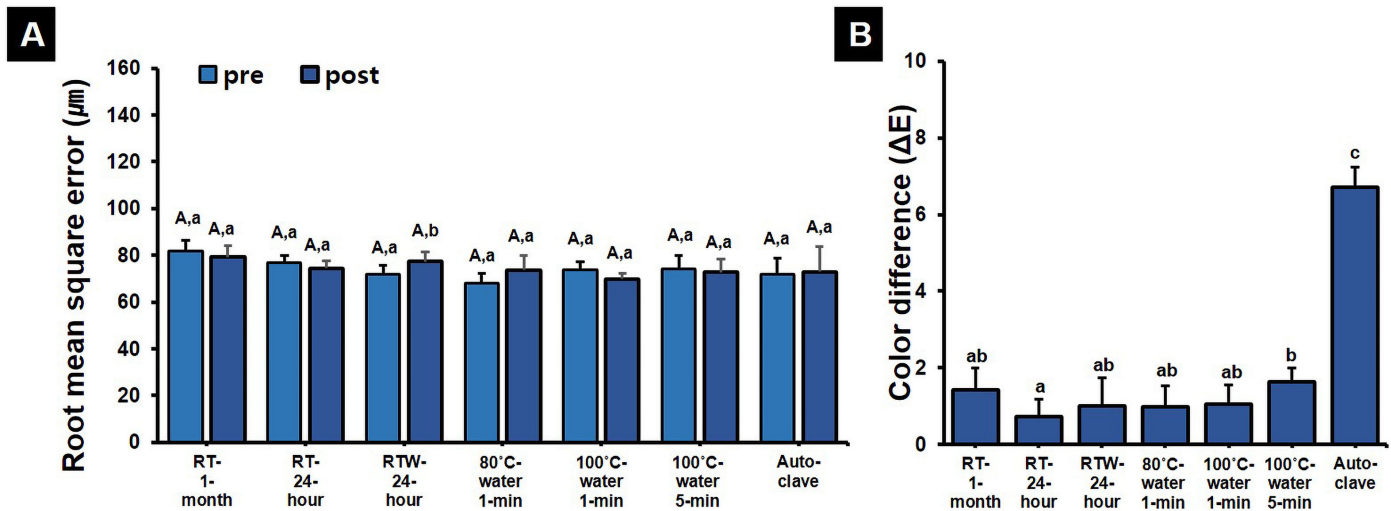


**Fig. 5.** Clinical property results. A) Trueness analysis performed by scanning the printed three-unit bridge and comparing it with the design file. B) Differences in color changes based on post-treatment method for the printed resin.

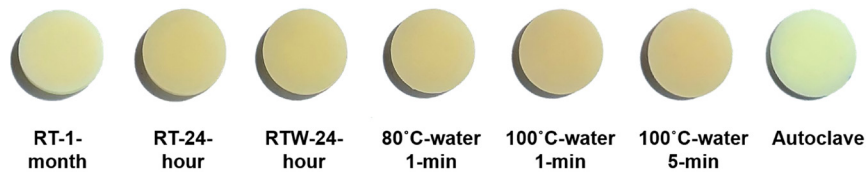


**Fig. 6.** Photographs of the qualitative color changes of the 3D-printed resins

group. This can be interpreted based on the results of Tsuchiya et al.[34], where denture resin immersed in water for 60 min was found to induce preleaching of formaldehyde and methyl methacrylate. This can be explained by the reduction in the concentration of toxic substances in the specimen, as residual monomers and compounds in the resin diffuse into water[43]. Compared with the specimens immersed in RTW and 80 °C water for 1 min, the cytotoxicity was significantly lower and the cell viability was significantly higher in the groups where the water temperature was high, such as the 100 °C-water 1-min, 100 °C-water 5-min, and autoclave groups. In addition, the cytotoxicity in the groups involving immersion in a water bath at 100 °C water for 1 min and 100 °C water for 5 min, and the autoclave group, did not increase even after 48 or 72 h. This was due to the increase in temperature, which improved the diffusion of residual monomers[32,33]. This may also be due to the reduction in toxic substances that result from the preleaching of resin compounds such as PI, monomers, additives, and residual monomers in aqueous media at high temperatures[20,34]. Another factor may be the hydrolysis of the residual monomers to methacrylic acid. Therefore, the increase in the biocompatibility of the printed resin samples in this study may have been caused by the diffusion and hydrolysis mechanism of toxic compounds into water. These results can also be interpreted as indicating that the treatment temperature strengthened the effect of the above mechanism. In a previous study by Park et al.[44], the effect of the chemical substances released from polymers and the physiological side effects of the products were tested. The author has mentioned the need for additional research using actual human gingival fibroblasts, and this study is noteworthy in that it confirms a

method for successfully reducing the toxicity of dental polymer resins to human gingival fibroblasts.

Fibroblasts are the most abundant cell types in connective tissue, have diverse functions, and produce complex cellular signaling networks by contacting other cells[45]. Gingival fibroblasts also play an essential role in wound healing, respond differently to growth factors, and produce matrix proteins for specific cells[46]. The CLSM images obtained in this study showed a significant effect of the heat treatment method on the biocompatibility of the printed resin, indicating clear differences in the shape, size, and number of cells. Well-developed morphology and increased cell adhesion were observed in the group in which the specimen was immersed in 80 °C water for 1 min, and the number of adherent cells significantly increased in the groups subjected to 100 °C water for 1 min, 100 °C water for 5 min, and autoclaving. These CLSM findings were consistent with those of the biocompatibility tests. The resins used in 3D printing contain UV-sensitive PIs, methacrylate monomers, fillers, and auxiliary compounds that exhibit cytotoxic effects[20,47]. Substances leached from these resin-based dental restorative materials have potentially negative effects on basic cellular functions, such as proliferation, metabolism, cell morphology, and cell membrane integrity[48]. Therefore, a simple and effective protocol to increase the biocompatibility of 3D-printed resin materials is required. The comprehensive results of the cell viability, cytotoxicity, and CLSM analyses obtained in this study demonstrate that immersing photocured resin in hot water can effectively improve cytocompatibility by inducing the preleaching of residual toxic substances[49].

Franz et al.[50] reported that DCs are essential for medical resin-based devices because they have a significant impact on biocompatibility. It has been reported that there is an inverse relationship between DC and the amount of residual monomer, that is, the higher the DC, the lower the amount of the residual monomer[43,51]. Leaching of residual monomers due to low DC can cause allergic reactions, such as local chemical irritation, hypersensitivity, and mucositis; therefore, it is necessary to improve DC[52–54]. A previous study reported that the glass transition of unpolymerized UDMA resin occurs at 90 °C[55]. Therefore, in this study, the DC was increased by applying heat above the glass transition temperature of the resin, and the heat-treatment method was designed by varying the temperature and time. An analysis of the DC of the specimens showed that it was affected by additional heat treatment, even after postcuring was complete. The DC was observed to have significantly increased in the groups whose specimens were further heated, namely, 80 °C-water 1-min and 100 °C-water 1-min groups. The highest DC, however, was obtained in the 100 °C-water 5-min group. These results were similar to those obtained from other methods of increasing the DC, such as heating in a drying box[56], microwave irradiation[57,58], and immersion in water at elevated temperatures[59,60]. The similarity in the results can be attributed to the fact that the polymerization rate of the resin was accelerated by heat. Increasing the temperature during resin polymerization enables better movement of the free radicals and development of polymer chains, thereby improving the monomer conversion rate and further polymerization[61–63]. From the results, it can also be observed that the decrease in the content and release of residual monomer in the resin significantly reduced the cytotoxicity[50,64]. The results of the FTIR analysis prove that the 100 °C-water 5-min method can be used as a simple method to increase the DC of the printed photopolymer resin while reducing the toxicity of the material. The residual monomer of the resin is temperature-dependent; however, because the resin is sensitive to high temperatures and pressure, it should be carried out within a range that does not affect the properties of the polymer.

The present analyses of the effects of the heat-treatment method on the volume changes in the 3D-printed three-unit bridge prostheses indicated that there were no significant differences between pre- and heat-treatment in all groups, except for the RTW-24-hour group. Several previous studies have compared and evaluated the dimensional accuracy of different 3D printing technologies, with errors of 0.20–0.50 mm defined as a clinically acceptable difference range[65–67]. The mean difference between the RMSE values before and after heat-treatment in the present RTW-24-hour group was approximately 5 µm, which was within the clinical tolerance range. Török et al. and Sharma et al.[68,69] autoclaved 3D-printed resin at a high temperature of 121 °C and analyzed the RMSE values of the specimens. Their results revealed no major deformations or structural changes, consistent with the trends identified in our study. The 3D-printed resin had a stable volume even after immersion in hot water at 80 °C and 100 °C when it was printed in the form of a three-unit bridge. This further supports the use of the hot water immersion method as a preleaching method. In this experiment, an analysis of the outer surface of a three-unit bridge was performed to evaluate its dimensional accuracy. However, additional studies, such as marginal fitness analysis, are required to analyze the prosthesis accuracy.

The color changes in the materials before and after heat treatment were quantitatively evaluated using a spectrophotometer[70]. A color difference ( $\Delta E_{00}$ ) value higher than 2.25 is considered clinically observable[70,71]. The color of the 3D-printed resin was indi-

cated to vary according to the heat-treatment method and in the 100 °C-water 1-min and 100 °C-water 5-min groups, the red hue increased in intensity; however, the color change in all groups other than the autoclave groups did not exceed the clinical acceptance threshold. The color difference in the autoclave group exceeded the clinically acceptable value of  $\Delta E_{00}$  2.25, which may be explained in several ways. Water absorption during the autoclave process may affect the color stability of the resin, and the water absorption of the 3D-printed resin may contribute to increasing the migration or adhesion of the pigments[72,73]. Therefore, it can be inferred that the increased water absorption potential of the 3D-printed resin during 20 min of autoclaving may have played a role in the observed color change. Another possible reason is the effect of the low inorganic filler content of the 3D-printed resin, which is necessary during the manufacturing process of 3D-printed objects because it maintains the resin viscosity as low as possible to facilitate the flow of the material and create a smooth surface[74]. However, a reduced filler content can lead to surface deterioration in the hydrothermal reaction process of the resin material and induce precipitation in the filler particles during storage[75]. These factors may have contributed to the increase in color change[74].

The flexural strength of the 3D-printed crown and bridge resin after heat treatment in the RT-24-hour group without any treatment was 133.8±18.4 MPa, whereas in the autoclave-treated group it was 95.3±16.9 MPa, which was a significant decrease. This indicates that the heat-treatment process exerted a strong effect on the flexural strength. These results are consistent with the decreased flexural strength found by Török et al.[68] for 3D-printed resin subjected to 121 °C steam sterilization. This decrease in the flexural strength can be attributed to several factors. Berli et al.[76] found that their 3D-printed resin group had significantly increased water absorption after thermal aging and that moisture adsorption significantly decreased the flexural strength and increased the deterioration of other mechanical properties. Another reason may be the monomer remaining in the resin, which could be induced by moisture absorption and swelling from the residual monomer, contributing to surface and mechanical property deterioration[77]. The Vickers hardness tests indicated that the flexural strength was not affected by heat treatment, with an average HV of approximately 20.9, which is similar to previous values found for 3D-printed crown and bridge materials[29]. This was also consistent with the results obtained by Török et al.[68], who found no significant difference in the Vickers hardness before and after dental surgical guided 3D-printed resin received steam sterilization at 121 °C.

One limitation of the present study is that only one type of 3D-printed resin was used in the experiments. Different types of printing equipment and resins produce different results. This study also used standardized specimens to quantify the biological and mechanical properties; therefore, the results for the final printed prosthesis may be different. Because environmental characteristics such as oral pH fluctuations, chewing, and the presence of bacteria and saliva were not considered in the present experiments, further corresponding standardized protocols and clinical studies are needed to strengthen our conclusions.

Within the limitations of this study, a method for lowering the cytotoxicity and increasing the cell viability of 3D-printed crowns and bridge resins was tested. Immersing printed resin samples in 100 °C water for 1 or 5 min after the curing process was an effective method for increasing the cytocompatibility by inducing preleach-



ing of toxic substances such as unpolymerized monomers, Pls, and additives. Simultaneously, it is possible to increase the DC by additional polymerization without affecting the flexural strength, surface hardness, or color changes of the material. This represents a suitable method for increasing the cytocompatibility of 3D printed photopolymer resin prostheses.

## 5. Conclusions

Within the limitations of this study, the following conclusions can be drawn:

1. The cell viability can be increased and cytotoxicity can be decreased by immersing a printed crown and bridge resin in 100 °C water for 1 or 5 min.
2. None of the applied heat-treatment methods affected the volume of 3D-printed three-unit bridge samples.
3. The heat-treatment method of immersing the printed resin in 100 °C water for 1 or 5 min can increase the DC without affecting the mechanical or optical stability of the printed resin.
4. Using an autoclave as a heat-treatment method decreases the flexural strength and increases the color differences.
5. None of the heat-treatment methods affected the Vickers hardness of the 3D-printed resin.

## Acknowledgements

This work was supported by the Korea Medical Device Development Fund grant funded by the Korea government (the Ministry of Science and ICT, the Ministry of Trade, Industry and Energy, the Ministry of Health & Welfare, the Ministry of Food and Drug Safety) (Project Number: 1711138524, KMDF\_PR\_20200901\_0245)

## Role of the funding source

This funding source had no role in the design of this study and will not have any role during its execution, analyses, interpretation of the data, or decision to submit the results.

## Conflict of interest statement

The authors have no conflicts of interest to declare. All co-authors have seen and agreed with the contents of the manuscript, and there are no financial interests to report. We certify that the submission is an original work and is not under review by any other publication.

## References

- [1] Beuer F, Schweiger J, Edelhoff D. Digital dentistry: an overview of recent developments for CAD/CAM generated restorations. *Br Dent J*. 2008;204:505–11. <https://doi.org/10.1038/sj.bdj.2008.350>, PMID:18469768
- [2] Alghazzawi TF. Advancements in CAD/CAM technology: options for practical implementation. *J Prosthodont Res*. 2016;60:72–84. <https://doi.org/10.1016/j.jpor.2016.01.003>, PMID:26935333
- [3] Bindl A, Mörmann WH. Marginal and internal fit of all-ceramic CAD/CAM crown-copings on chamfer preparations. *J Oral Rehabil*. 2005;32:441–7. <https://doi.org/10.1111/j.1365-2842.2005.01446.x>, PMID:15899023
- [4] Lin WS, Harris BT, Zandinejad A, Morton D. Use of digital data acquisition and CAD/CAM technology for the fabrication of a fixed complete dental prosthesis on dental implants. *J Prosthet Dent*. 2014;111:1–5. <https://doi.org/10.1016/j.prosdent.2013.04.010>, PMID:24189115
- [5] Berman B. 3-D printing: the new industrial revolution. *Bus Horiz*. 2012;55:155–62. <https://doi.org/10.1016/j.bushor.2011.11.003>
- [6] Edelhoff D, Beuer F, Schweiger J, Brix O, Stimmelmayer M, Guth JF. CAD/CAM-generated high-density polymer restorations for the pretreatment of complex cases: a case report. *Quintessence Int*. 2012;43:457–67. PMID:22532953
- [7] van Noort R. The future of dental devices is digital. *Dent Mater*. 2012;28:3–12. <https://doi.org/10.1016/j.dental.2011.10.014>, PMID:22119539
- [8] Khaleli AA, Farzin M, Akhlaghian M, Pardis S, Mir N. Evaluation of the marginal fit of metal copings fabricated by using 3 different CAD-CAM techniques: Milling, stereolithography, and 3D wax printer. *J Prosthet Dent*. 2020;124:81–6. <https://doi.org/10.1016/j.prosdent.2019.09.002>, PMID:31672421
- [9] Baumann M, Dickens P, Tuck C, Hague R. The cost of additive manufacturing: machine productivity, economies of scale and technology-push. *Technol Forecast Soc Change*. 2016;102:193–201. <https://doi.org/10.1016/j.techfore.2015.02.015>
- [10] Lin HH, Lonic D, Lo LJ. 3D printing in orthognathic surgery – A literature review. *J Formos Med Assoc*. 2018;117:547–58. <https://doi.org/10.1016/j.jfma.2018.01.008>, PMID:29398097
- [11] Simoneti DM, Pereira-Cenci T, dos Santos MBF. Comparison of material properties and biofilm formation in interim single crowns obtained by 3D printing and conventional methods. *J Prosthet Dent*. 2020;127:168–72. <https://doi.org/https://doi.org/10.1016/j.prosdent.2020.06.026>, PMID:33168174
- [12] Duarte S Jr, Sartori N, Phark JH. Ceramic-reinforced polymers: CAD/CAM hybrid restorative materials. *Curr Oral Health Rep*. 2016;3:198–202. <https://doi.org/10.1007/s40496-016-0102-2>
- [13] Sigusch BW, Pflaum T, Völpe A, Schinkel M, Jandt KD. The influence of various light curing units on the cytotoxicity of dental adhesives. *Dent Mater*. 2009;25:1446–52. <https://doi.org/10.1016/j.dental.2009.06.016>, PMID:19647309
- [14] Moharamzadeh K, Van Noort R, Brook IM, Scutt AM. Cytotoxicity of resin monomers on human gingival fibroblasts and HaCat keratinocytes. *Dent Mater*. 2007;23:40–4. <https://doi.org/10.1016/j.dental.2005.11.039>, PMID:16426672
- [15] Meglioli M, Naveau A, Macaluso GM, Catros S. 3D printed bone models in oral and cranio-maxillofacial surgery: a systematic review. *3D Print Med*. 2020;6:30. <https://doi.org/10.1016/j.dental.2005.11.039>
- [16] Steyrer B, Neubauer P, Liska R, Stampfl J. Visible light photoinitiator for 3D-printing of tough methacrylate resins. *Materials (Basel)*. 2017;10:1445. <https://doi.org/10.3390/ma10121445>, PMID:29257107
- [17] Leonhardt S, Klare M, Scheer M, Fischer T, Cordes B, Eblenkamp M. Biocompatibility of photopolymers for additive manufacturing. *Curr Dir Biomed Eng*. 2016;2:113–6. <https://doi.org/10.1515/cdbme-2016-0028>
- [18] Hwang HJ, Lee SJ, Park EJ, Yoon HI. Assessment of the trueness and tissue surface adaptation of CAD-CAM maxillary denture bases manufactured using digital light processing. *J Prosthet Dent*. 2019;121:110–7. <https://doi.org/10.1016/j.prosdent.2018.02.018>, PMID:30006217
- [19] Pianelli C, Devaux J, Bebelman S, Leloup G. The micro-Raman spectroscopy, a useful tool to determine the degree of conversion of light-activated composite resins. *J Biomed Mater Res*. 1999;48:675–81. [https://doi.org/10.1002/\(SICI\)1097-4636\(1999\)48:5<675::AID-JBM11>3.0.CO;2-P](https://doi.org/10.1002/(SICI)1097-4636(1999)48:5<675::AID-JBM11>3.0.CO;2-P), PMID:10490681
- [20] Carve M, Wlodkowic D. 3D-Printed Chips: Compatibility of Additive Manufacturing Photopolymeric Substrata with Biological Applications. *Micromachines (Basel)*. 2018;9:91. <https://doi.org/10.3390/mi9020091>, PMID:30393367
- [21] Reinert KH. Aquatic toxicity of acrylates and methacrylates: quantitative structure-activity relationships based on Kow and LC50. *Regul Toxicol Pharmacol*. 1987;7:384–9. [https://doi.org/10.1016/0273-2300\(87\)90059-6](https://doi.org/10.1016/0273-2300(87)90059-6), PMID:3438503
- [22] Dearfield KL, Millis CS, Harrington-Brock K, Doerr CL, Moore MM. Analysis of the genotoxicity of nine acrylate/methacrylate compounds in L5178Y mouse lymphoma cells. *Mutagenesis*. 1989;4:381–93. <https://doi.org/10.1093/mutage/4.5.381>, PMID:2687634
- [23] Oskui SM, Diamante G, Liao C, Shi W, Gan J, Schlenk D, et al. Assessing and reducing the toxicity of 3D-printed parts. *Environ Sci Technol Lett*. 2016;3:1–6. <https://doi.org/10.1021/acs.estlett.5b00249>
- [24] Schuster GS, Lefebvre CA, Dirksen TR, Knoernschild KL, Caughman GB. Relationships between denture base resin cytotoxicity and cell lipid metabolism. *Int J Prosthodont*. 1995;8:580–6. PMID:8595119
- [25] Cimpan MR, Matre R, Cressey LI, Tysnes B, Lie SA, Gjertsen BT, et al.; Mihaela Roxana Cimpan, Roald Matre. The effect of heat- and auto-polymerized denture base polymers on clonogenicity, apoptosis, and necrosis in fibroblasts: denture base polymers induce apoptosis and necrosis. *Acta Odontol Scand*. 2000;58:217–28. <https://doi.org/10.1080/000163500750051773>, PMID:11144873

- [26] Kim SH, Watts DC. Degree of conversion of bis-acrylic based provisional crown and fixed partial denture materials. *J Korean Acad Prosthodont*. 2008;46:639–43. <https://doi.org/10.4047/jkap.2008.46.6.639>
- [27] Papanu JS, Hess DW, Soane DS, Bell AT. Swelling of poly(methyl methacrylate) thin films in low molecular weight alcohols. *J Appl Polym Sci*. 1990;39:803–23. <https://doi.org/10.1002/app.1990.070390404>
- [28] Xu Y, Xepapadeas AB, Koos B, Geis-Gerstorfer J, Li P, Spintzyk S. Effect of post-rinsing time on the mechanical strength and cytotoxicity of a 3D printed orthodontic splint material. *Dent Mater*. 2021;37:e314–27. <https://doi.org/10.1016/j.dental.2021.01.016>, PMID:33610310
- [29] Kim D, Shim JS, Lee D, Shin SH, Nam NE, Park KH, et al. Effects of Post-Curing Time on the Mechanical and Color Properties of Three-Dimensional Printed Crown and Bridge Materials. *Polymers (Basel)*. 2020;12:2762. <https://doi.org/10.3390/polym12112762>, PMID:33238528
- [30] Macdonald NP, Zhu F, Hall CJ, Reboud J, Crosier PS, Patton EE, et al. Assessment of biocompatibility of 3D printed photopolymers using zebrafish embryo toxicity assays. *Lab Chip*. 2016;16:291–7. <https://doi.org/10.1039/C5LC01374G>, PMID:26646354
- [31] Kreß S, Schaller-Ammann R, Feiel J, Priedl J, Kasper C, Egger D. 3D Printing of Cell Culture Devices: Assessment and Prevention of the Cytotoxicity of Photopolymers for Stereolithography. *Materials (Basel)*. 2020;13:3011. <https://doi.org/10.3390/ma13133011>, PMID:32640644
- [32] Lamb DJ, Ellis B, Priestley D. Loss into water of residual monomer from autopolymerizing dental acrylic resin. *Biomaterials*. 1982;3:155–9. [https://doi.org/10.1016/0142-9612\(82\)90005-9](https://doi.org/10.1016/0142-9612(82)90005-9), PMID:7115859
- [33] Shim JS, Watts DC. Residual monomer concentrations in denture-base acrylic resin after an additional, soft-liner, heat-cure cycle. *Dent Mater*. 1999;15:296–300. [https://doi.org/10.1016/S0109-5641\(99\)00048-2](https://doi.org/10.1016/S0109-5641(99)00048-2), PMID:10551098
- [34] Tsuchiya H, Hoshino Y, Tajima K, Takagi N. Leaching and cytotoxicity of formaldehyde and methyl methacrylate from acrylic resin denture base materials. *J Prosthet Dent*. 1994;71:618–24. [https://doi.org/10.1016/0022-3913\(94\)90448-0](https://doi.org/10.1016/0022-3913(94)90448-0), PMID:8040827
- [35] Standardization IOF. Dentistry-Polymer-based Filling, Restorative and Luting Materials. Global Engineering Documents; 2000.
- [36] Standardization IOF. Dentistry: polymer-based crown and bridge materials. ISO 1992;10477:1992 (E).
- [37] Poggio C, Lombardini M, Gaviati S, Chiesa M. Evaluation of Vickers hardness and depth of cure of six composite resins photo-activated with different polymerization modes. *J Conserv Dent*. 2012;15:237–41. <https://doi.org/10.4103/0972-0707.97946>, PMID:22876009
- [38] Ozsoy U. Comparison of Different Calculation Methods Used to Analyze Facial Soft Tissue Asymmetry: Global and Partial 3-Dimensional Quantitative Evaluation of Healthy Subjects. *J Oral Maxillofac Surg*. 2016;74:1847.e1–9. <https://doi.org/10.1016/j.joms.2016.05.012>, PMID:27292525
- [39] Bayarsaikhan E, Lim JH, Shin SH, Park KH, Park YB, Lee JH, et al. Effects of Postcuring Temperature on the Mechanical Properties and Biocompatibility of Three-Dimensional Printed Dental Resin Material. *Polymers (Basel)*. 2021;13:1180. <https://doi.org/10.3390/polym13081180>, PMID:33916899
- [40] Lin CH, Lin YM, Lai YL, Lee SY. Mechanical properties, accuracy, and cytotoxicity of UV-polymerized 3D printing resins composed of Bis-EMA, UDMA, and TEGDMA. *J Prosthet Dent*. 2020;123:349–54. <https://doi.org/10.1016/j.prosdent.2019.05.002>, PMID:31202550
- [41] Wataha JC, Rueggeberg FA, Lapp CA, Lewis JB, Lockwood PE, Ergle JW, et al. In vitro cytotoxicity of resin-containing restorative materials after aging in artificial saliva. *Clin Oral Investig*. 1999;3:144–9. <https://doi.org/10.1007/s007840050093>, PMID:10803126
- [42] Saxena P, Pant AB, Gupta SK, Pant V. Release and toxicity of dental resin composite. *Toxicol Int*. 2012;19:225–34. <https://doi.org/10.4103/0971-6580.103652>, PMID:23293458
- [43] Vallittu PK, Miettinen V, Alakuijala P. Residual monomer content and its release into water from denture base materials. *Dent Mater*. 1995;11:338–42. [https://doi.org/10.1016/0109-5641\(95\)80031-X](https://doi.org/10.1016/0109-5641(95)80031-X), PMID:8595832
- [44] Park JH, Lee H, Kim JW, Kim JH. Cytocompatibility of 3D printed dental materials for temporary restorations on fibroblasts. *BMC Oral Health*. 2020;20:157. <https://doi.org/10.1186/s12903-020-01150-2>, PMID:32487153
- [45] Willershausen-Zönnchen B, Lemmen C, Hamn G. Influence of high glucose concentrations on glycosaminoglycan and collagen synthesis in cultured human gingival fibroblasts. *J Clin Periodontol*. 1991;18:190–5. <https://doi.org/10.1111/j.1600-051X.1991.tb01132.x>, PMID:2061419
- [46] Fawzy El-Sayed KM, Paris S, Becker ST, Neuschl M, Buhr W, Sälzer S, et al. Periodontal regeneration employing gingival margin-derived stem/progenitor cells: an animal study. *J Clin Periodontol*. 2012;39:861–70. <https://doi.org/10.1111/j.1600-051X.2012.01904.x>, PMID:22694281
- [47] Schmelzer E, Over P, Gridelli B, Gerlach JC. Response of primary human bone marrow mesenchymal stromal cells and dermal keratinocytes to thermal printer materials in vitro. *J Med Biol Eng*. 2016;36:153–67. <https://doi.org/10.1007/s40846-016-0118-z>, PMID:27231463
- [48] Bakopoulou A, Papadopoulos T, Garefis P. Molecular toxicology of substances released from resin-based dental restorative materials. *Int J Mol Sci*. 2009;10:3861–99. <https://doi.org/10.3390/ijms10093861>, PMID:19865523
- [49] Ngan CGY, O'Connell CD, Blanchard R, Boyd-Moss M, Williams RJ, Bourke J, et al. Optimising the biocompatibility of 3D printed photopolymer constructs in vitro and in vivo. *Biomed Mater*. 2019;14:035007. <https://doi.org/10.1088/1748-605X/ab09c4>, PMID:30795002
- [50] Franz A, König F, Lucas T, Watts DC, Schedle A. Cytotoxic effects of dental bonding substances as a function of degree of conversion. *Dent Mater*. 2009;25:232–9. <https://doi.org/10.1016/j.dental.2008.07.003>, PMID:18774602
- [51] Vallittu PK, Ruyter IE, Buykuilmaz S. Effect of polymerization temperature and time on the residual monomer content of denture base polymers. *Eur J Oral Sci*. 1998;106:588–93. <https://doi.org/10.1046/j.0909-8836.1998.eos106109.x>, PMID:9527360
- [52] Hochman N, Zalkind M. Hypersensitivity to methyl methacrylate: mode of treatment. *J Prosthet Dent*. 1997;77:93–6. [https://doi.org/10.1016/S0022-3913\(97\)70214-2](https://doi.org/10.1016/S0022-3913(97)70214-2), PMID:9029473
- [53] Giunta J, Zablotsky N. Allergic stomatitis caused by self-polymerizing resin. *Oral Surg Oral Med Oral Pathol*. 1976;41:631–7. [https://doi.org/10.1016/0030-4220\(76\)90315-7](https://doi.org/10.1016/0030-4220(76)90315-7), PMID:1063962
- [54] Gonçalves TS, Morganti MA, Campos LC, Rizzato SMD, Menezes LM. Allergy to auto-polymerized acrylic resin in an orthodontic patient. *Am J Orthod Dentofacial Orthop*. 2006;129:431–5. <https://doi.org/10.1016/j.ajodo.2005.10.017>, PMID:16527642
- [55] Nguyen JF, Pomes B, Sadoun M, Richaud E. Curing of urethane dimethacrylate composites: A glass transition study. *Polym Test*. 2019;80:106113. <https://doi.org/10.1016/j.polymertesting.2019.106113>
- [56] Boeckler A, Morton D, Poser S, Dette K. Release of dibenzoyl peroxide from polymethyl methacrylate denture base resins: an in vitro evaluation. *Dent Mater*. 2008;24:1602–7. <https://doi.org/10.1016/j.dental.2008.03.019>, PMID:18471871
- [57] Vallittu PK. The effect of surface treatment of denture acrylic resin on the residual monomer content and its release into water. *Acta Odontol Scand*. 1996;54:188–92. <https://doi.org/10.3109/00016359609003522>, PMID:8811142
- [58] Yunus N, Harrison A, Huggett R. Effect of microwave irradiation on the flexural strength and residual monomer levels of an acrylic resin repair material. *J Oral Rehabil*. 1994;21:641–8. <https://doi.org/10.1111/j.1365-2842.1994.tb01179.x>, PMID:7830199
- [59] Urban VM, Machado AL, Vergani CE, Giampaolo ET, Pavarina AC, de Almeida FG, et al. Effect of water-bath post-polymerization on the mechanical properties, degree of conversion, and leaching of residual compounds of hard chairside relined resins. *Dent Mater*. 2009;25:662–71. <https://doi.org/10.1016/j.dental.2008.10.017>, PMID:19135715
- [60] Urban VM, Machado AL, Vergani CE, Jorge EG, Santos LPS, Leite ER, et al. Degree of conversion and molecular weight of one denture base and three relined resins submitted to post-polymerization treatments. *Mater Res*. 2007;10:191–7. <https://doi.org/10.1590/S1516-14392007000200016>
- [61] Daronch M, Rueggeberg FA, De Goes MF. Monomer conversion of pre-heated composite. *J Dent Res*. 2005;84:663–7. <https://doi.org/10.1177/154405910508400716>, PMID:15972598
- [62] Park SH, Lee CS. The difference in degree of conversion between light-cured and additional heat-cured composites. *Oper Dent*. 1996;21:213–7. PMID:9484175
- [63] Ahn KH, Lim S, Kum KY, Chang SW. Effect of preheating on the viscoelastic properties of dental composite under different deformation conditions. *Dent Mater J*. 2015;34:702–6. <https://doi.org/10.4012/dmj.2015-042>, PMID:26438995
- [64] Durner J, Obermaier J, Draenert M, Ilie N. Correlation of the degree of conversion with the amount of elutable substances in nano-hybrid dental composites. *Dent Mater*. 2012;28:1146–53. <https://doi.org/10.1016/j.dental.2012.08.006>, PMID:22940188

- [65] Wan Hassan WN, Yusoff Y, Mardi NA. Comparison of reconstructed rapid prototyping models produced by 3-dimensional printing and conventional stone models with different degrees of crowding. *Am J Orthod Dentofacial Orthop.* 2017;151:209–18. <https://doi.org/10.1016/j.ajodo.2016.08.019>, PMID:28024776
- [66] Hazeveld A, Huddleston Slater JJR, Ren Y. Accuracy and reproducibility of dental replica models reconstructed by different rapid prototyping techniques. *Am J Orthod Dentofacial Orthop.* 2014;145:108–15. <https://doi.org/10.1016/j.ajodo.2013.05.011>, PMID:24373661
- [67] Bell A, Ayoub A, Siebert P. Assessment of the accuracy of a three-dimensional imaging system for archiving dental study models. 2003;30:219–23. <https://doi.org/https://doi.org/10.1093/ortho/30.3.219>, PMID:14530419
- [68] Török G, Gombocz P, Bognár E, Nagy P, Dinya E, Kispélyi B, et al. Effects of disinfection and sterilization on the dimensional changes and mechanical properties of 3D printed surgical guides for implant therapy – pilot study. *BMC Oral Health.* 2020;20:19. <https://doi.org/10.1186/s12903-020-1005-0>, PMID:31973705
- [69] Sharma N, Cao S, Msallem B, Kunz C, Brantner P, Honigsmann P, et al. Effects of Steam Sterilization on 3D Printed Biocompatible Resin Materials for Surgical Guides—An Accuracy Assessment Study. *J Clin Med.* 2020;9:1506. <https://doi.org/10.3390/jcm9051506>, PMID:32429549
- [70] Ghinea R, Pérez MM, Herrera LJ, Rivas MJ, Yebra A, Paravina RD. Color difference thresholds in dental ceramics. *J Dent.* 2010;38(suppl 2):e57–64. <https://doi.org/10.1016/j.jdent.2010.07.008>, PMID:20670670
- [71] Özarslan MM, Büyükkaplan UŞ, Barutçigil Ç, Arslan M, Türker N, Barutçigil K. Effects of different surface finishing procedures on the change in surface roughness and color of a polymer infiltrated ceramic network material. *J Adv Prosthodont.* 2016;8:16–20. <https://doi.org/10.4047/jap.2016.8.1.16>, PMID:26949483
- [72] Imirzalioglu P, Karacaer O, Yilmaz B, Ozmen MSc I. Color stability of denture acrylic resins and a soft lining material against tea, coffee, and nicotine. *J Prosthodont.* 2010;19:118–24. <https://doi.org/10.1111/j.1532-849X.2009.00535.x>, PMID:20002978
- [73] Dietschi D, Campanile G, Holz J, Meyer JM. Comparison of the color stability of ten new-generation composites: an in vitro study. *Dent Mater.* 1994;10:353–62. [https://doi.org/10.1016/0109-5641\(94\)90059-0](https://doi.org/10.1016/0109-5641(94)90059-0), PMID:7498599
- [74] Gruber S, Kamnoedboon P, Özcan M, Srinivasan M. CAD/CAM Complete Denture Resins: An In Vitro Evaluation of Color Stability. *J Prosthodont.* 2021;30:430–9. <https://doi.org/10.1111/jopr.13246>, PMID:32864812
- [75] Kessler A, Reymus M, Hickel R, Kunzelmann KH. Three-body wear of 3D printed temporary materials. *Dent Mater.* 2019;35:1805–12. <https://doi.org/10.1016/j.dental.2019.10.005>, PMID:31727446
- [76] Berli C, Thieringer FM, Sharma N, Müller JA, Dedem P, Fischer J, et al. Comparing the mechanical properties of pressed, milled, and 3D-printed resins for occlusal devices. *J Prosthet Dent.* 2020;124:780–6. <https://doi.org/10.1016/j.prosdent.2019.10.024>, PMID:31955837
- [77] Engler MLPD, Güth JF, Keul C, Erdelt K, Edelhoff D, Liebermann A. Residual monomer elution from different conventional and CAD/CAM dental polymers during artificial aging. *Clin Oral Investig.* 2020;24:277–84. <https://doi.org/10.1007/s00784-019-02947-4>, PMID:31098712



This is an open-access article distributed under the terms of Creative Commons Attribution-NonCommercial License 4.0 (CC BY-NC 4.0), which allows users to distribute and copy the material in any format as long as credit is given to the Japan Prosthodontic Society. It should be noted however, that the material cannot be used for commercial purposes.